Contrasting Rainfall Thresholds for Landslide Initiation: A Multi-Temporal Analysis of the 2014 and 2018 Disasters in Hiroshima, Japan

Kumari M. A.K. * , Tsuyoshi Wakatsuki , Chiaki T. Oguchi , Osada Masahiko

Posted Date: 15 April 2026

doi: 10.20944/preprints202604.0975.v1

Keywords: landslide early-warning systems; landslide prediction; multi-temporal rainfall analysis; rainfall intensity–duration threshold; rainfall-induced landslides

 doi:10.20944/preprints202604.0975.v1

Article

Contrasting Rainfall Thresholds for Landslide Initiation: A Multi-Temporal Analysis of the 2014 and 2018 Disasters in Hiroshima, Japan

Kumari M.A.K. [1,*], Tsuyoshi Wakatsuki [2], Chiaki T. Oguchi [3] and Osada Masahiko [4]

[1] Graduate School of Science and Engineering, Saitama University, 255 Shimo-Okubo, Sakura-ku, Saitama, 338-8570, Japan
[2] Storm, Flood, and Landslide Research Division, National Research Institute for Earth Science and Disaster Resilience, 3-1 Tennodai, Tsukuba, Ibaraki, 305-0006, Japan
[3] Department of Civil and Environmental Engineering, School of Environmental and Society, Institute of Science Tokyo, 4259-G3-11, Nagatsuta, Midori-ku, Yokohama 226-8501, Japan
[4] Department of Civil and Environmental Engineering, Saitama University, 255 Shimo-Okubo, Sakura-ku, Saitama, 338-8570, Japan
* Correspondence: kanchanamallikaarachchi@gmail.com

Abstract

Rainfall is the mainly trigger of landslides in Japan, especially in mountainous regions with steep slopes and highly weathered terrain. This study examines rainfall conditions linked to landslides in Hiroshima Prefecture by analyzing multi-temporal precipitation data and establishing thresholds for the 2014 and 2018 disasters. Rainfall events were identified from satellite data using an inter-event dry-period. Intensity–duration (I–D) relationships, percentile thresholds, and Receiver Operating Characteristic analysis were used to assess rainfall thresholds. Additionally, topographic threshold analysis was preformed to evaluate how slope gradient and lithology influence rainfall-induced landslides. The results reveal notable differences in the triggering mechanisms between the two disasters. The 2014 landslides were caused by short-duration, intense rainfall (376 mm over about 40 hours), while the 2018 event resulted from prolonged rainfall exceeding 1000 mm over more than 11 days. I–D thresholds suggest that the 2014 event was primarily triggered by high intensity, whereas the 2018 event was driven by long duration. Landslides occurred most frequently on moderate to steep slopes, and lower triggering thresholds were observed in granitic terrain. These findings highlight that both rainfall features and terrain conditions jointly influence landslide occurrence, emphasizing the need to incorporate both factors into rainfall-based early-warning systems.

Keywords: landslide early-warning systems; landslide prediction; multi-temporal rainfall analysis; rainfall intensity–duration threshold; rainfall-induced landslides

1. Introduction

Intense rainfall events are the most significant natural triggers of geohazards worldwide, often causing floods, debris flows, and landslides [1,2]. Among these hazards, landslides are the most destructive geomorphic processes, leading to substantial economic losses, environmental damage, and human casualties [3,4]. They commonly occur in mountainous and hilly regions where steep slopes, complex geological conditions, and heavy precipitation combined to create favorable conditions for slope instability [5,6]. Rainfall-induced landslides make up a significant proportion of slope failures in many areas, underscoring the importance of understanding their triggering mechanisms and enhancing predictive capabilities [7,8].

The term landslide generally refers to the downslope movement of soil, rock, or debris caused by gravity [9,10]. Although landslides may be triggered by earthquakes, volcanic activity, and human

 doi:10.20944/preprints202604.0975.v1

disturbances, rainfall remains one of the most common triggers, especially for shallow landslides and debris flows [11–13]. Rainfall-induced landslides usually occur when infiltration raising pore water pressure and decreasing the shear strength of slope materials, which eventually causes slope failure [11]. This process is influenced by several hydrometeorological factors, including rainfall intensity, duration, and prior precipitation conditions.

Considerable research has centered on understanding the complex relationship between rainfall and landslide initiation. Numerous studies have shown that landslide occurrence is often linked to critical rainfall conditions that surpass certain hydrological thresholds [14,15]. In particular, rainfall intensity and duration are key factors in controlling slope stability. Short-duration, high-intensity rainfall can rapidly saturate near-surface soils and trigger shallow landslides, while prolonged rainfall may gradually increase groundwater levels and promote deeper slope failures [5,16]. Antecedent rainfall conditions significantly affect soil moisture buildup and hydrological response, which can make slopes more susceptible to failure during subsequent rainfall events [11,14].

The importance of rainfall-induced landslide research has increased under climate change, which is expected to intensify extreme precipitation events in many regions of the world [17]. These changes may significantly elevate landslide hazards in mountainous areas where slope stability is already highly sensitive to rainfall variability. Consequently, improving prediction of rainfall-induced landslides has become a key priority in disaster risk reduction and environmental management.

Japan is especially vulnerable to rainfall-induced landslides because of its complex geological structure, steep mountainous terrain, and high annual rainfall. About seventy percent of the Japanese archipelago is mountainous, and the country is situated within the tectonically active Pacific Ring of Fire. Combined with seasonal monsoons and frequent typhoons, these conditions create a highly vulnerable environment for slope failure. As a result, landslides happen often across Japan, frequently causing serious socio-economic impacts such as loss of life, damage to infrastructure and homes, disruption of transportation, and large economic losses.

Several catastrophic rainfall events in Japan have shown the destructive impact of rainfall-induced landslides. For example, the Hiroshima landslide disaster in 2014 and the heavy rainfall in western Japan in 2018 triggered thousands of landslides across large mountainous areas, causing widespread damage and fatalities. These disasters emphasize the urgent need for better landslide forecasting systems that can identify critical rainfall conditions before failures happen. Additionally, recent studies indicate that rainfall thresholds derived from one event may not be fully transferable to another specially under changing climatic conditions [18]. Rainfall threshold models have become one of the most widely used tools for landslide prediction. They define critical rainfall levels that must be exceeded for landslides to happen [14].

Numerous empirical rainfall thresholds have been developed using historical landslide inventories and meteorological data. Among these methods, intensity–duration (I–D) relationships are commonly used to describe the minimum rainfall intensity needed to trigger landslides for a specific rainfall duration [14,19]. These models have been effectively applied in many regions worldwide and form the foundation of several operational landslide early warning systems [20]. In Japan, rainfall threshold models have also been created using historical disaster records and rainfall observations, proving their effectiveness in predicting landslide events [21].

Rainfall thresholds are heavily influenced by local environmental conditions and can vary greatly between regions. Several factors determine the amount of rainfall needed to trigger landslides, including lithology, soil properties, vegetation cover, slope gradient, hydrological conditions, and mean annual rainfall [15,20]. These factors affect infiltration, groundwater movement, and slope stability, thereby shaping the rainfall conditions required for slope failure. Therefore, thresholds developed in one setting may not be directly applicable elsewhere without proper calibration.

Besides rainfall patterns, topographic and geomorphological factors also strongly influence landslide occurrence. Terrain features such as slope angle, curvature, and contributing area affect the distribution of gravitational forces and surface runoff, which then impact slope stability and landslide

 doi:10.20944/preprints202604.0975.v1

susceptibility [7]. Combining rainfall data with topographic parameters is expected to improve the spatial and physical realism of landslide prediction models.

Despite significant progress in rainfall threshold modeling, several key limitations still exist in current research. Many studies have concentrated on single rainfall events or region-specific datasets, which can restrict the overall applicability and robustness of the thresholds derived [14,20]. In addition, most investigations rely primarily on intensity–duration threshold relationships, which may oversimplify the complex interactions between rainfall characteristics and terrain conditions [15,20]. Comparisons of different threshold estimation methods are still limited, and the performance of various statistical approaches has not been fully assessed. Techniques like percentile-based thresholds and receiver operating characteristic (ROC) curve analysis have shown potential in hazard prediction studies, but their use and comparison in rainfall-induced landslide prediction remain underexplored. Furthermore, rainfall thresholds are often developed without sufficiently incorporating topographic controls, even though terrain conditions strongly influence where slope failure occurred.

In Japan, relatively few studies have explored how the rainfall–landslide relationship varies over time across multiple disaster events. This is a critical issue because extreme rainfall events are becoming more frequents and may produce different triggering mechanisms over time. Comparative analysis of multiple rainfall disasters can therefore improve understanding of threshold variability and support the development of more reliable early-warning criteria.

To address these gaps, this study explores rainfall-induced landslides in Hiroshima Prefecture by combining multi-temporal rainfall data with topographic parameters from two major disaster events. The study evaluates rainfall thresholds using percentile-based methods, ROC curve–based optimal thresholds, empirical intensity, duration relationships, and further examine how slope gradient and lithology influence landslide occurrence. By comparing threshold behaviors across the 2014 and 2018 events, this research aims to clarify the relative role of rainfall characteristic and terrain conditions in landslide initiation.

The findings may offer valuable insights to improve understanding of rainfall-triggered landslide in Japan and provide more robust basis for rainfall-based early-warning systems and hazard mitigation planning.

2. Study Area

The study area is located in Hiroshima Prefecture, western Honshu, Japan, a region highly prone to rainfall-induced landslides because of its steep mountainous terrain, heavily weathered granitic bedrock, and frequent intense rainfall events. The present study concentrates on areas impacted by two major rainfall-triggered landslide disasters that occurred in 2014 and 2018 in Hiroshima (Figure 1).

 doi:10.20944/preprints202604.0975.v1

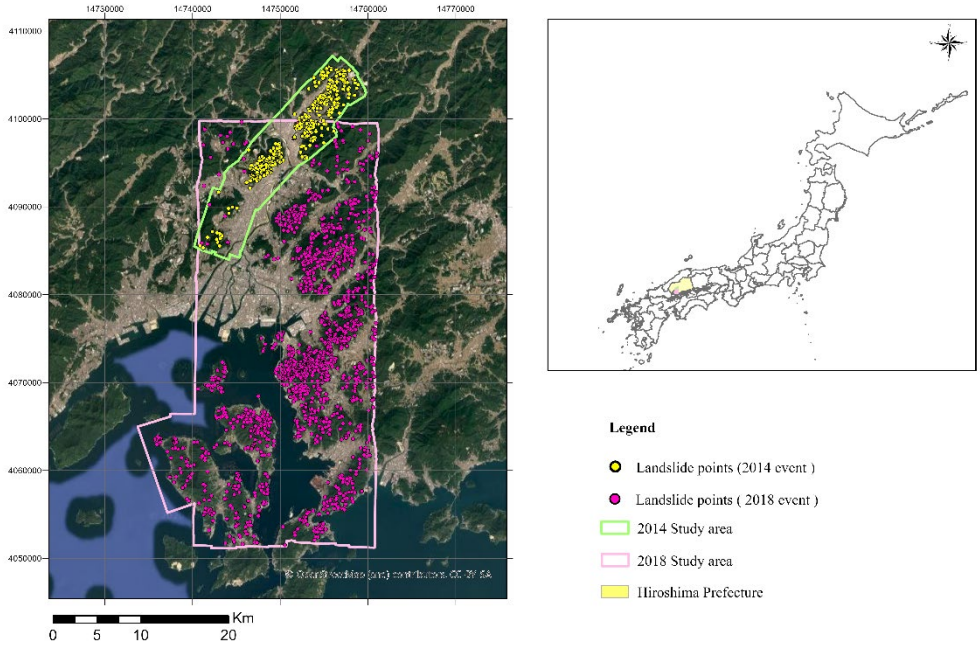

Figure 1. Location of the study areas in Hiroshima Prefecture showing the regions affected by the 2014 and 2018 rainfall-induced landslide disasters.

This region has experienced several catastrophic rainfall-induced landslides over the past decades. On August 20, 2014, short-duration rainfall triggered numerous slope failures and debris flows in northern Hiroshima City, causing severe damage to residential areas located at the foot of slopes [22–25]. According to the Ministry of Land, Infrastructure, Transport and Tourism (MLIT), the disaster resulted in 74 fatalities and the complete destruction of 133 houses [26,27]. In contrast, July 2018 western Japan heavy rainfall disaster produced prolonged rainfall over much larger area and triggered sediment-related disasters across the Hiroshima prefecture, resulted in 151 deaths, 5 people missing, and the complete destruction of 1,176 houses [25,28,29].

The region has experienced similar catastrophic events in the past. In June 1999, a severe rainstorm triggered more than 7,000 shallow landslides in the mountainous areas west of Hiroshima City, leading to 32 deaths [30,31]. The recurrence of such events shows that the Hiroshima region remains vulnerable to rainfall-induced landslides. These disasters highlight the contrasting role of short, high-intensity rainfall and long-term, cumulative rainfall in landslide initiation [25].

Two separate but partially overlapping study areas were defined corresponding to the 2014 and 2018 landslide events. The 2014 area covers approximately 100.40 km², while the 2018 area covers705.35 km². The 2014 study area is lies between 34°24′35.28″-34°35′34.8″ N and 132°24′46.8″ - 132°36′36″ E, whereas 2018 study area extends from 34°9′57.24″-34°31′32.88″ N and 132°21′24.84″ - 132°36′9″ E. Landslide density is relatively high across of the 2018 area, except in the northwestern region.

Topographically, the study area is mostly mountainous, with elevations reaching about 900 meters, steep slopes, narrow valleys, and highly dissected drainage networks. These conditions increase surface runoff concentration and slope saturation during heavy rainfall. Geologically, the area is primarily composed of Late Cretaceous granitic rocks, mainly consist of biotite granite and hornblende–biotite granodiorite, with minor pebbly mudstone welded tuff units (Figure 2). Granite rocks are especially important because deep chemical weathering in humid climates produce thick regolith layers that are highly vulnerable to failure during heavy rain [31,32]. Most landslide in the 2014 event originated as shallow failures in weatherd granite and rapidly transformed into debris flows [31].

 doi:10.20944/preprints202604.0975.v1

Overall, the combination of steep terrain, weathered granitic bedrock, and frequent heavy rainfall makes Hiroshima an ideal location for investigating rainfall thresholds and landslide triggering conditions.

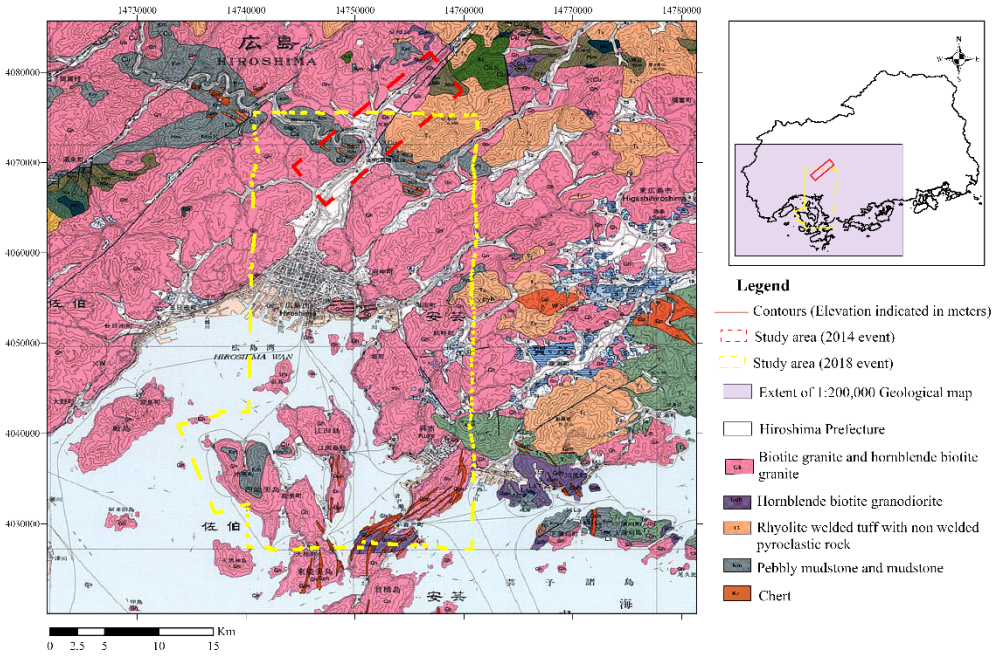

Figure 2. Geological map of the study area in Hiroshima Prefecture showing the spatial distribution of landslides triggered during the 2014 and 2018 rainfall disasters (Modified after 1:200,000 geology map of Hiroshima, 1986).

3. Materials and Methodology

3.1. Landslide Inventory Preparation

This study focuses on two rainfall-induced landslide disasters that occurred in Hiroshima Prefecture, Japan, during the August 2014 and July 2018 extreme rainfall events. Two separates but partially overlapping study areas were defined corresponding to these disasters (Figure 1). Both events were triggered by intense and prolonged rainfall that caused widespread shallow landslides and debris flows, resulting in significant damage to infrastructure and loss of life.

A detailed landslide inventory was prepared using post-event high-resolution ortho-photographs and field verification. The ortho-photographs for the 2014 disaster were obtained from a Grant-in-Aid for Scientific Research project titled “Research on the actual situation of the debris flow disaster that occurred in Hiroshima City due to heavy rain in August 2014 and disaster prevention measures” [34]. The ortho-photographs for the 2018 disaster were obtained from a project conducted by the Geospatial Information Authority of Japan titled “Heavy rain disaster caused by Typhoon No.7 and fronts in July 2018 (Hirodori-zaka area)”.

Landslide initiation zones were identified through visual interpretation of high-resolution aerial photographs with a ground resolution of 5 cm. The interpretation process focused on detecting geomorphic signatures indicative of recent slope failures, including exposed soil surfaces, disrupted vegetation, head scarps, and linear debris flow tracks downslope. Such visual indicators are commonly used in landslide mapping and have been widely applied in geomorphological studies [35,36].

Landslide polygons were manually delineated using the Editor tools in ArcGIS by tracing the boundaries of disturbed surfaces and identifying the head scarp regions representing failure initiation points. This approach allows accurate identification of landslide source areas and

 doi:10.20944/preprints202604.0975.v1

minimizes positional uncertainty in inventory preparation [37]. A total of 600 landslide initiation points were mapped for the 2014 event whereas, 1960 initiation points were mapped for the 2018 event (Figure 2). Selected locations were verified through field observations and cross-checked with published disaster investigation reports to improve the reliability of the inventory.

3.2. Rainfall Data and Pre-Processing

Rainfall data were obtained from the observation network operated by the Japan Meteorological Agency (JMA). The agency has approximately 1,579 surface observation stations across Japan, including 156 manned meteorological stations and a dense automated monitoring system known as the Automated Meteorological Data Acquisition System (AMeDAS). In addition to ground-based measurements, this study utilized radar–gauge composite rainfall data known as Analytical Rainfall, which integrates observations from weather radar and rain gauge stations to produce spatially distributed rainfall estimates. Analytical rainfall data are provided as hourly rainfall distribution datasets covering the entire country with a spatial resolution of 1 km.

3.3. Rainfall Event Definition

Individual rainfall events were identified using the Inter-Event Dry Period (IEDP) approach [38]. This method separates rainfall events based on the length of dry intervals between consecutive rainfall periods. A rainfall event is considered to end when rainfall ceases for a specified duration exceeding the defined dry period threshold [20]. In this study, an IEDP of 12–24 hours was adopted following recommendations from previous rainfall threshold studies [39]. Under this criterion, rainfall sequences separated by a dry period of 12 or 24 hours were treated as independent rainfall events. For each rainfall event, the following parameters were calculated: rainfall start time, rainfall end time, rainfall duration (hours), and cumulative rainfall (mm). In addition, cumulative rainfall totals were calculated for multiple antecedent periods (1 h, 2 h, 6 h, 12 h, 24 h, and 48 h) in order to analyze rainfall conditions preceding landslide initiation (Figure 3)

Preprints.org (www.preprints.org) | NOT PEER-REVIEWED | Posted: 15 April 2026 doi:10.20944/preprints202604.0975.v1

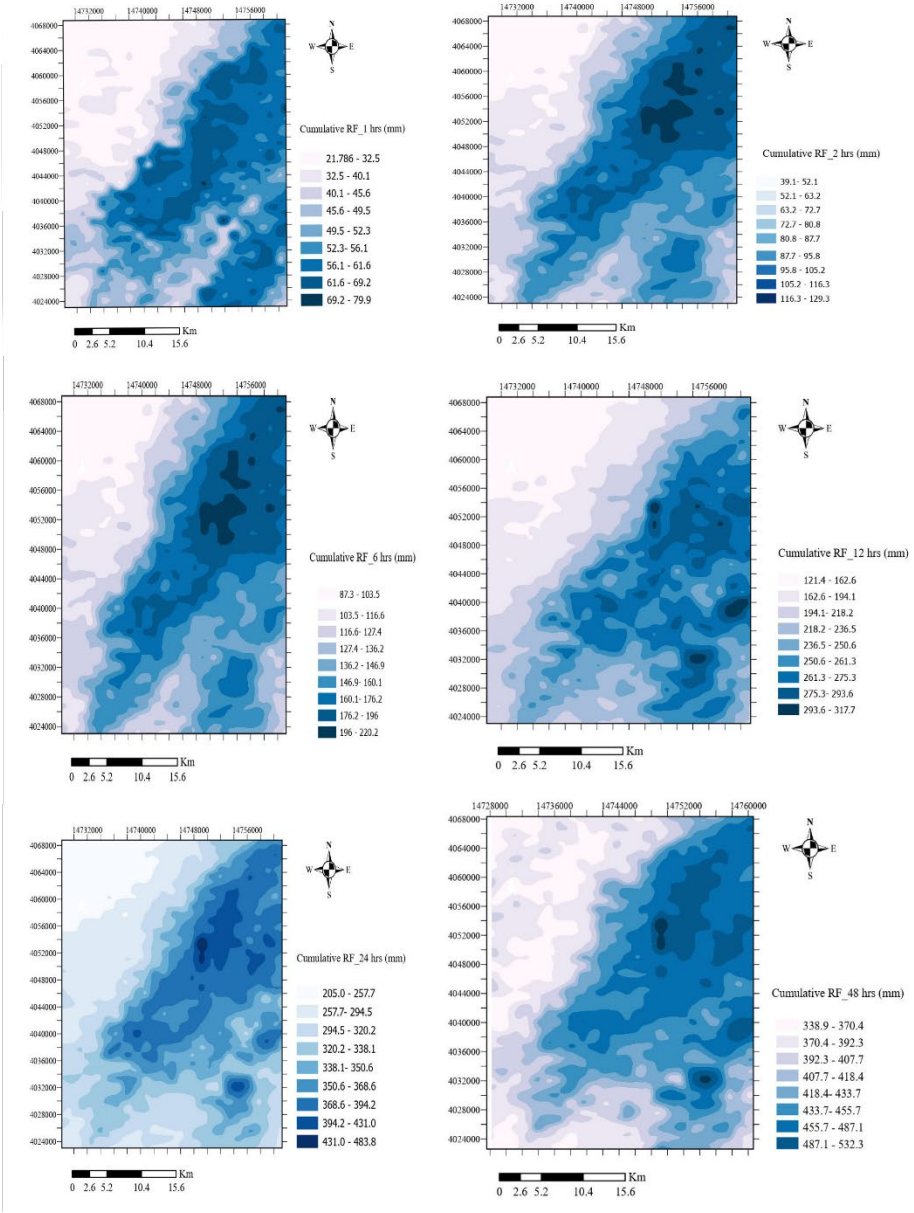

Figure 3. (a) 1hr cumulative rainfall, (b) 2hr cumulative rainfall, (c) 6hr cumulative rainfall, (d) 12hr cumulative rainfall, (e) 24hr cumulative rainfall and (f) 48hr cumulative rainfall.

3.4. Rainfall Threshold Estimation

Rainfall thresholds represent critical rainfall conditions that are capable of triggering landslides [20,40]. These thresholds are commonly expressed using an intensity–duration (I–D) relationship of the form:

$$I = aD^{-b} \quad (1)$$

where I represent rainfall intensity (mm h^{-1}), D represents rainfall duration (h), and a and b are empirical parameters derived through regression analysis.

Several threshold estimation approaches were considered in this study to determine the rainfall conditions responsible for landslide initiation. These approaches include percentile-based thresholds, ROC curve analysis, empirical intensity–duration thresholds, and topographic rainfall thresholds. The percentile-based threshold approach estimates rainfall thresholds by identifying rainfall intensity values corresponding to specific percentiles of landslide-triggering rainfall events. This method allows identification of rainfall levels above which landslides are more likely to occur. The

 doi:10.20944/preprints202604.0975.v1

ROC-based threshold approach evaluates the predictive performance of rainfall thresholds by comparing true positive and false positive rates. This method identifies the optimal rainfall threshold that maximizes landslide detection accuracy while minimizing false alarms.

The empirical intensity–duration (I–D) method involves plotting rainfall intensity against rainfall duration on a logarithmic scale and fitting a lower-bound regression line that represents the minimum rainfall conditions required for landslide initiation. This approach has been widely used in landslide studies worldwide [16].

In addition to rainfall analysis, a topographic threshold analysis was conducted to incorporate the influence of terrain conditions and geomorphological factors in defining landslide-triggering conditions. Landslide initiation is strongly controlled by local slope characteristics such as slope gradient, relief, and surface morphology, which determine the balance between gravitational driving forces and resisting forces on hillslopes [10]. Previous studies have shown that integrating topographic parameters with rainfall information improves the reliability of rainfall threshold estimation for landslide initiation [14,20].

In this study, slope angle derived from the digital elevation model (DEM) was classified into five slope classes: <10°, 10–20°, 21–30°, 31–40°, and >40°, which were assigned numerical classes (0–4) for statistical analysis. For each slope class, landslide occurrence data were analyzed to evaluate the relationship between slope gradient and landslide area, allowing identification of the slope conditions under which landslides most frequently occur. Similar slope-based classifications have been widely used in landslide susceptibility and threshold studies to represent terrain controls on slope instability [35,41].

Rainfall thresholds were then calculated for each slope class using rainfall variables of different durations (1-hr, 2-hr, 6-hr, 12-hr, 24-hr, and 48-hr). The threshold rainfall for each class was defined using the upper percentile (e.g., 90th percentile) of rainfall values associated with recorded landslide events, representing the rainfall conditions most commonly associated with slope failures within each slope category. The use of statistical or empirical rainfall thresholds derived from landslide inventories has been widely adopted in landslide early-warning and hazard assessment studies [14,42].

To further investigate the role of geological conditions, the analysis was extended to different lithological units. Landslide occurrences were grouped according to lithology, and rainfall thresholds were recalculated separately for each combination of slope class and lithological unit. Lithology influences mechanical strength, permeability, and weathering characteristics of rocks, which in turn control slope morphology and susceptibility to rainfall-induced failures [43,44]. By comparing rainfall thresholds across lithological units, it is possible to assess how geological conditions indirectly influence landslide occurrence through their control on terrain evolution, slope configuration, and hydrological response. This integrated approach enables a more comprehensive understanding of the interaction between rainfall, topography, and lithology in controlling rainfall-triggered landslides.

3.5. Comparison with Existing Rainfall Thresholds for Japan

To evaluate the derived rainfall thresholds, the results were compared with previously proposed intensity–duration relationships developed for landslides in Japan. Several studies have established empirical rainfall thresholds based on historical landslide datasets.

For example, the threshold proposed by Jibson 1989 for global landslide events is expressed as [45]:

$$I = 39.71D^{-0.62} \quad (2)$$

Similarly, Hong et al.,2005 proposed an empirical rainfall threshold for landslides based on satellite rainfall data [46]:

$$I = 1.35 + 55D^{-1.00} \quad (3)$$

 doi:10.20944/preprints202604.0975.v1

A regional rainfall threshold for landslides in Japan was also proposed by Saito et al., 2010 based on long-term landslide and rainfall observations [47]:

$$I = 2.18D^{-0.26} \quad (4)$$

These previously established thresholds were plotted together with the rainfall conditions associated with the 2014 and 2018 landslide events in order to evaluate whether the rainfall characteristics of the studied disasters confirms the existing empirical relationships.

4. Results

4.1. Rainfall Event Identification

4.1.1. Identification of Rainfall Events for the 2014 Hiroshima Landslide Disaster

Rainfall events associated with the landslide disaster of 20 August 2014 were identified using satellite-derived half-hourly rainfall data for 117 locations. These events were divided using an inter-event dry period (IEDP) criterion in which a rainfall event begins when hourly rainfall exceeds 4 mm and ends when rainfall remains below 4 mm for six consecutive hours. This definition is consistent with approaches used to identify short-duration, high-intensity rainfall events that frequently trigger shallow landslides.

Only the rainfall records before the disaster data were retained. Eight distinct rainfall events were identified between 7 August and 20 August 2014 (Table 1).

Table 1. Rainfall events identified prior to the 20th August 2014 Hiroshima landslide disaster.

Rainfall event	Start Time (Date & time)	End Time (Date & time)	Duration (hours)	Total Rainfall (mm)
1	8/7/14 14:30	8/7/14 15:30	1	0.24
2	8/8/14 1:00	8/10/14 17:30	64.5	105.76
3	8/11/14 10:30	8/11/14 14:00	3.5	0.27
4	8/12/14 6:00	8/12/14 7:00	1	0.75
5	8/13/14 11:00	8/13/14 15:30	4.5	1.17
6	8/14/14 8:00	8/17/14 9:30	73.5	114.18
7	8/17/14 23:00	8/18/14 19:00	20	3.26
8	8/19/14 3:30	8/20/14 20:00	40.5	376.05

The identified rainfall events exhibit considerable variability in duration and accumulated rainfall. Short-duration events occurred on 7 August, 11 August, 12 August, and 13 August, with durations ranging from 1 to 4.5 hours and total rainfall below 2 mm. These events represent routine rainfall episodes with limited hydrological impact. In contrast, several prolonged rainfall events were observed. The event from 8 August to 10 August lasted 64.5 hours with approximately 105.76 mm of accumulated rainfall, while another event from 14 August to 17 August persisted for 73.5 hours, producing 114.18 mm of rainfall. These prolonged rainfall periods likely contributed to progressive soil moisture accumulation and slope saturation.

The most significant rainfall event occurred between 19 August 03:30 and 20 August 20:00, lasting 40.5 hours and generating 376.05 mm of rainfall. This event exhibits both high cumulative rainfall and moderate duration, representing the most hydrologically significant rainfall episode prior to the disaster.

Overall, the rainfall pattern indicates a transition from relatively moderate precipitation earlier in the month to extreme rainfall immediately preceding the landslide disaster. The clustering of rainfall events within a two-week period suggests cumulative hydrological effects that may have contributed to progressive slope instability.

 doi:10.20944/preprints202604.0975.v1

4.1.2. Identification of Rainfall Events for the 2018 Western Japan Landslide Disaster

Rainfall events associated with the July 2018 Western Japan rainfall disaster were identified using satellite-derived half-hourly rainfall data for 1225 locations. The same rainfall event definition based on a 24-hour inter-event dry period was applied to ensure consistency with previous studies.

Five rainfall events were identified between June and July 2018 (Table 2). These events are characterized by considerable variability in rainfall duration and magnitude.

Table 2. Rainfall events identified prior to the July 2018 Western Japan landslide disaster.

Rainfall event	Start Time (Date & time)	End Time (Date & time)	Duration (hours)	Total Rainfall (mm)
1	6/5/18 9:30	6/12/18 18:00	176.5	139.72
2	6/14/18 21:30	6/16/18 9:00	35.5	10.49
3	6/17/18 11:00	6/21/18 8:30	93.5	163.01
4	6/23/18 0:30	6/23/18 21:30	21	9.71
5	6/26/18 10:00	7/7/18 23:30	277.5	1031.62

The first rainfall event occurred between 5 June and 12 June, lasting 176.5 hours with approximately 139.72 mm of accumulated rainfall. A second event from 14 June to 16 June lasted 35.5 hours and produced 10.49 mm of rainfall. A third rainfall event occurred between 17 June and 21 June, with a duration of 93.5 hours and 163.01 mm of rainfall. These early events indicate prolonged but relatively moderate rainfall conditions during June. The most significant rainfall event occurred between 26 June and 7 July 2018, continuing for 277.5 hours (approximately 11.5 days) and producing 1031.62 mm of rainfall. This event represents an extreme long-duration rainfall episode and corresponds to the rainfall period responsible for the widespread landslide disasters across western Japan.

The duration of this rainfall event coincides with previously reported disaster periods from 28 June to 8 July 2018, as documented in previous studies [29]. Overall, the rainfall pattern in 2018 is characterized by extremely long-duration precipitation with large cumulative rainfall, indicating persistent atmospheric moisture supply and sustained precipitation conditions.

4.2. Intensity–Duration (I–D) Rainfall Thresholds

Rainfall intensity–duration (I–D) thresholds were derived for the landslide-triggering rainfall events associated with the 2014 and 2018 disasters. The thresholds were obtained by fitting a power-law relationship between rainfall intensity (I) and rainfall duration (D).

For the 2014 disaster event, the derived threshold relationship is:

$$I = 95D^{-0.57} \quad (5)$$

For the 2018 disaster event, the derived threshold relationship is:

$$I = 61.76D^{-0.47} \quad (6)$$

The resulting threshold curves are presented in Figure 4. In both cases, rainfall intensity decreases with increasing rainfall duration, indicating an inverse relationship between the two variables. The 2014 threshold exhibits relatively higher rainfall intensity values for shorter durations compared with the 2018 threshold. The derived intensity–duration (I–D) rainfall thresholds were compared with previously proposed landslide-triggering thresholds for Japan, including those of Jibson (1989), Hong et al. (2005), and Saito et al. (2010) [45–47]. These thresholds were plotted alongside rainfall conditions from the 2014 and 2018 disaster events (Figure 5) to evaluate their consistency with established empirical relationships

Preprints.org (www.preprints.org) | NOT PEER-REVIEWED | Posted: 15 April 2026 doi:10.20944/preprints202604.0975.v1

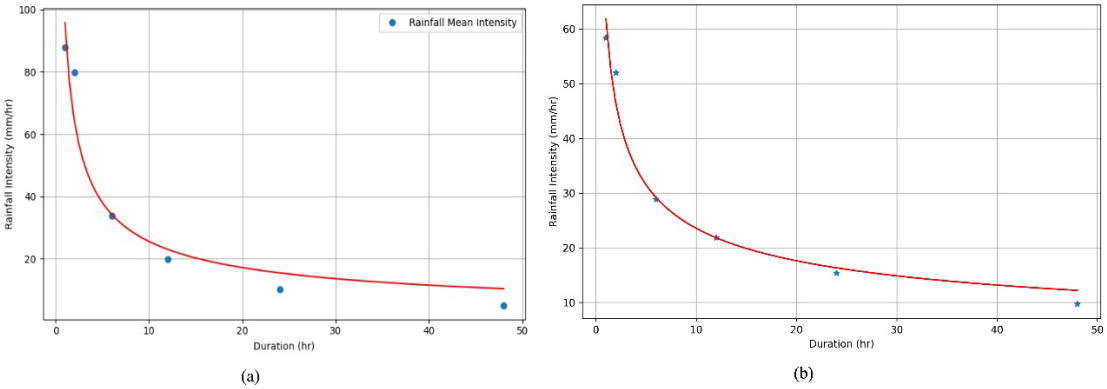

Figure 4. Rainfall intensity–duration (I–D) threshold derived for (a) the 2014 Hiroshima landslide disaster (b) 2018 disaster.

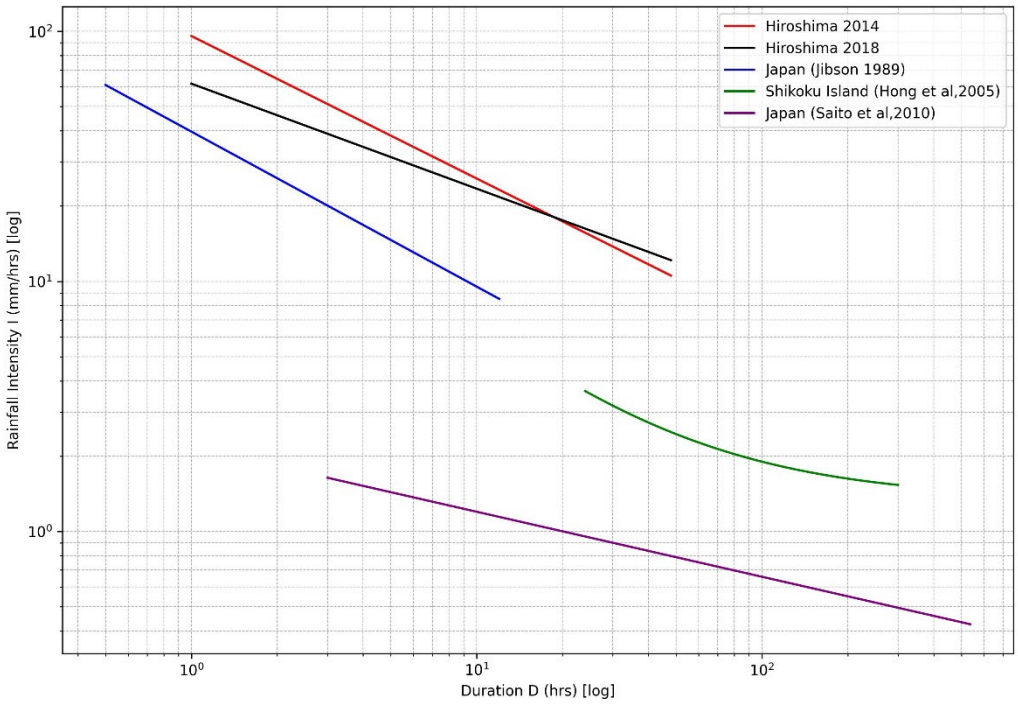

Figure 5. Comparison of the derived rainfall intensity–duration thresholds for the 2014 and 2018 events with previously proposed landslide rainfall thresholds.

4.3. Percentile-Based Rainfall Thresholds

Rainfall thresholds were also estimated using a percentile-based approach. Rainfall intensities corresponding to the 90th, 95th, and 99th percentiles were calculated for several rainfall durations (1, 2, 6, 12, 24, and 48 hours) for both disaster events.

The calculated percentile thresholds are summarized in Table 3.

Table 3. Percentile-based rainfall thresholds (90th, 95th, and 99th percentiles) for different rainfall durations for the 2014 and 2018 landslide events.

	90% rainfall threshold (mm)		95% rainfall threshold (mm)		99% rainfall threshold (mm)	
Rainfall index	**2014**	**2018**	**2014**	**2018**	**2014**	**2018**

 doi:10.20944/preprints202604.0975.v1

1 hour	103.76	64.32	108.54	65.7	113.77	66.8
2 hours	181.15	117.59	188.12	119.11	200.12	125.35
6 hours	224.57	194.87	231.4	198.65	246.32	202.86
12 hours	262.77	280.28	269.87	286.31	284.45	294.95
24 hours	265.93	395.33	273.37	403.68	287.81	409.6
48 hours	268.86	496.25	275.81	505.77	290.05	520.33

For the 2014 event, the 90th percentile rainfall threshold ranged from 103.76 mm for 1-hour rainfall to 268.86 mm for 48-hour rainfall while the 99th percentile threshold ranged from 113.77 mm (1 hour) to 290.05 mm (48 hours). For the 2018 event, the 90th percentile rainfall threshold ranged from 64.32 mm for 1-hour rainfall to 496.25 mm for 48-hour rainfall the 99th percentile rainfall threshold ranged from 66.8 mm (1 hour) to 520.33 mm (48 hours). The variation of percentile-based rainfall thresholds across different durations is illustrated in Figure 6.

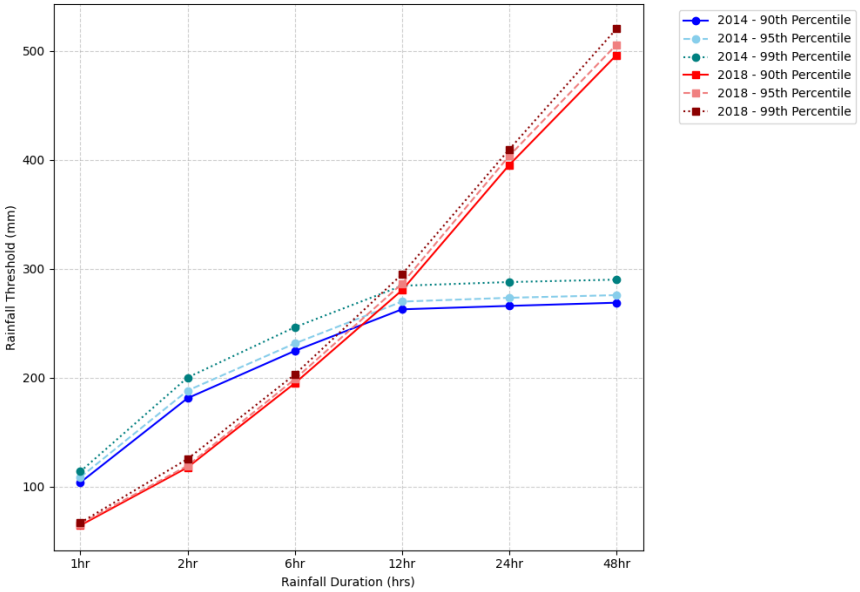

Figure 6. Percentile-based rainfall thresholds for different rainfall durations for the 2014 and 2018 landslide events.

4.4. ROC-Based Rainfall Threshold Analysis

ROC analysis was conducted to evaluate the predictive performance of rainfall thresholds for landslide occurrence. The predictive ability of rainfall indices for different durations was assessed using the Area Under the Curve (AUC) metric.

The ROC analysis results are summarized in Table 4.

Table 4. ROC-based rainfall thresholds and corresponding AUC values for different rainfall durations for the 2014 and 2018 disaster events.

Rainfall index	2014 Event		2018 Event	
	AUC value	RF threshold (mm)	AUC value	RF threshold (mm)
1 hour	0.60	68.12	0.67	54.79
2 hours	0.61	132.97	0.69	94.96
6 hours	0.57	171.3	0.66	166.62
12 hours	0.53	211	0.68	257.87
24 hours	0.52	215.29	0.67	368.51
48 hours	0.52	218.5	0.66	462.83

 doi:10.20944/preprints202604.0975.v1

For the 2014 event, AUC values ranged from 0.52 to 0.61 across different rainfall durations. The highest AUC value was observed for 2-hour rainfall (AUC = 0.61) with a corresponding rainfall threshold of 132.97 mm. For the 2018 event, AUC values ranged from 0.66 to 0.69. The highest predictive performance was observed for 2-hour rainfall (AUC = 0.69) with a rainfall threshold of 94.96 mm.

The ROC curves for the rainfall indices are shown in Figures 7 and 8.

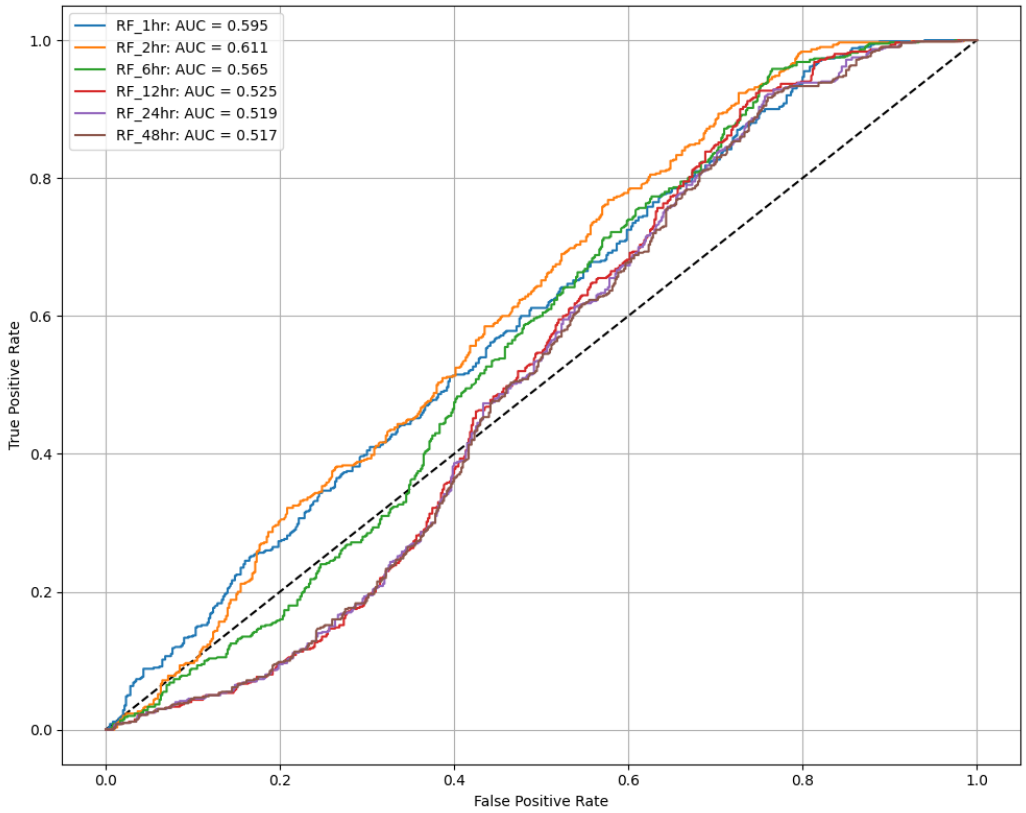

Figure 7. ROC curves showing the performance of rainfall thresholds for different rainfall durations during the 2014 disaster event.

 doi:10.20944/preprints202604.0975.v1

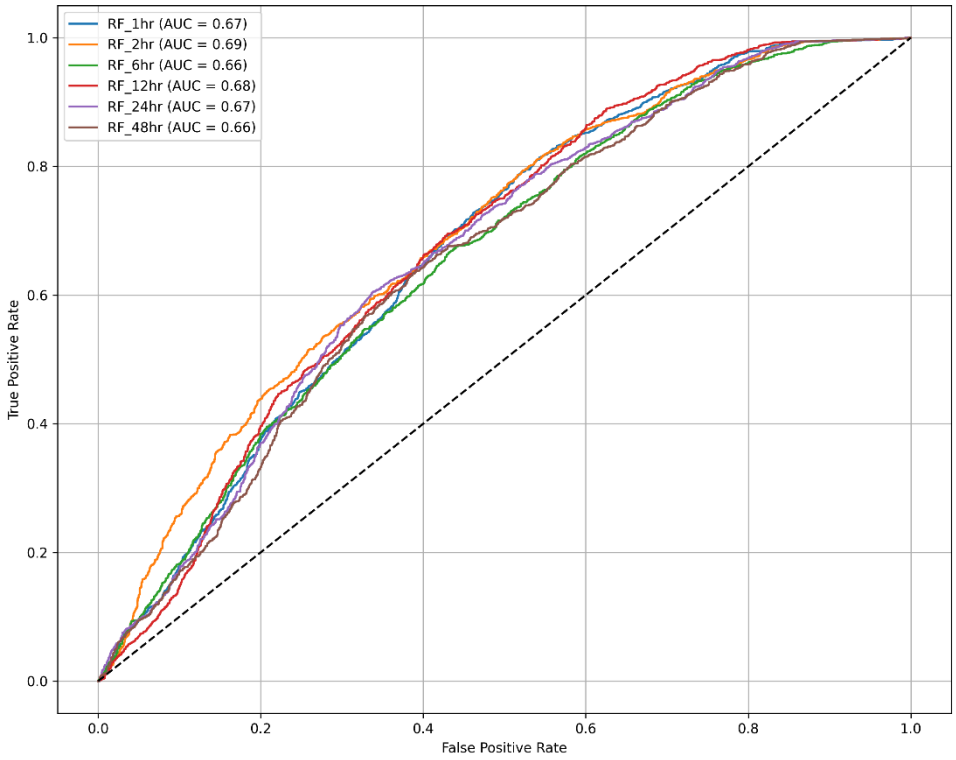

Figure 8. ROC curves showing the performance of rainfall thresholds for different rainfall durations during the 2018 disaster event.

4.5. Topographic Threshold

4.5.1. Rainfall Thresholds for Different Slope Classes

The statistical analysis of slope angle across the defined slope classes (<10°, 10–20°, 21–30°, 31–40°, and >40°) indicates clear differentiation in terrain characteristics associated with landslide occurrences. Since no landslides were recorded on slopes <10°, the analysis mainly considers slope classes 1–4. The mean slope angle increase consistently with slope class, ranging from 16.9° in slope class 1 to 44.4° in slope class 4, confirming the validity of the slope classification scheme.

Rainfall threshold analysis using the 90th percentile of rainfall associated with landslide events exhibits systematic variation across slope classes (Figure 9). For short-duration rainfall, the 1-hour rainfall threshold increases from 66.9 mm in slope class 1 to 93.7 mm in slope class 3, indicating that steeper slopes generally require slightly higher rainfall intensities to initiate landslides.

 doi:10.20944/preprints202604.0975.v1

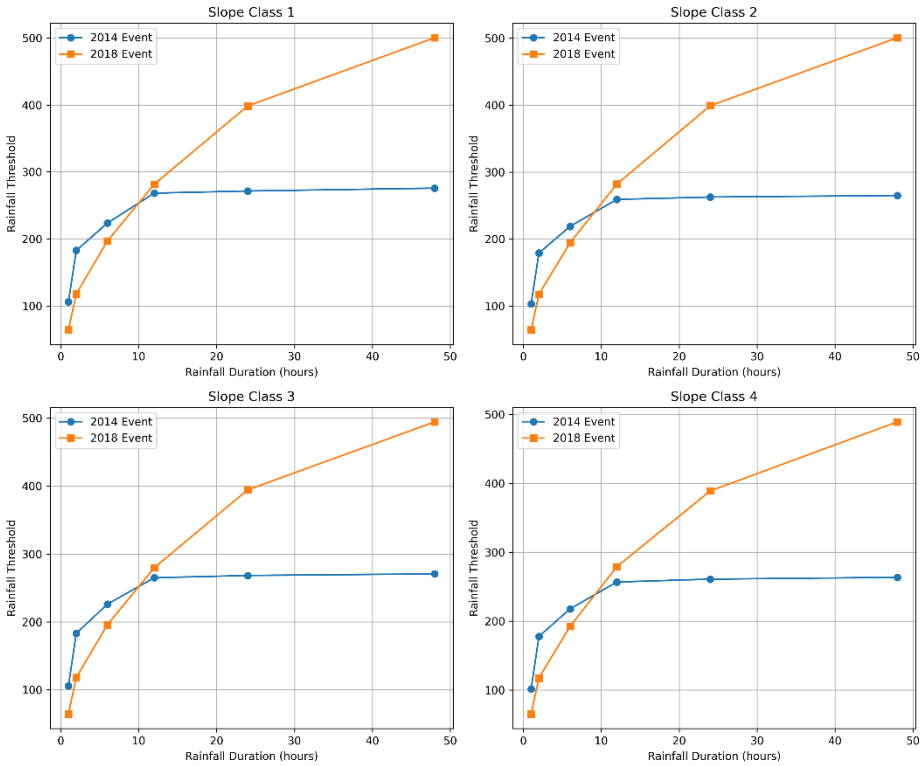

Figure 9. Rainfall threshold curves for different slope classes derived from the 2014 and 2018 landslide events. The plots show rainfall intensity–duration relationships for slope classes 1–4, illustrating differences in rainfall conditions associated with landslide initiation between the two events.

Similarly, the 2-hour rainfall threshold increases from 123.8 mm to 171.5 mm between slope classes 1 and 3. For longer rainfall durations, the thresholds show relatively small variation between slope classes. The 24-hour rainfall threshold ranges from approximately 397 mm to 385 mm, while the 48-hour threshold ranges from approximately 498 mm to 485 mm. These results suggest that short-duration rainfall intensity is more sensitive to slope gradient, whereas long-duration rainfall thresholds remain relatively uniform across different slope classes.

4.5.2. Rainfall Thresholds Considering Slope Class and Lithology

The spatial distribution of landslides across lithological units reveals significant variation in the relationship between slope angle and landslide area (Figure 10). Landslides were observed in several rock types, including granite, dike granite porphyry, mudstone, mudstone intercalated with acid tuff layers, rhyolite, chert, and granodiorite.

When rainfall thresholds are calculated separately for each lithological unit and slope class, pronounced differences emerge. In general, dike granite porphyry shows relatively low short-duration rainfall thresholds, with 1-hour thresholds ranging from 55.4 mm to 61.8 mm across slope classes. Granite shows slightly higher thresholds, typically around 66–89 mm for 1-hour rainfall, reflecting somewhat greater resistance to rainfall-induced slope failure. Mudstone units exhibit even higher short-duration rainfall thresholds (approximately 90–95 mm), although their thresholds for longer rainfall durations are comparatively lower. Volcanic rocks such as rhyolite show the highest rainfall thresholds, with 1-hour rainfall values exceeding 108–111 mm, suggesting that stronger lithologies require higher rainfall intensities to trigger slope failures. These variations demonstrate that lithological conditions significantly influence rainfall thresholds, highlighting the importance of incorporating geological factors into rainfall-induced landslide analysis.

 doi:10.20944/preprints202604.0975.v1

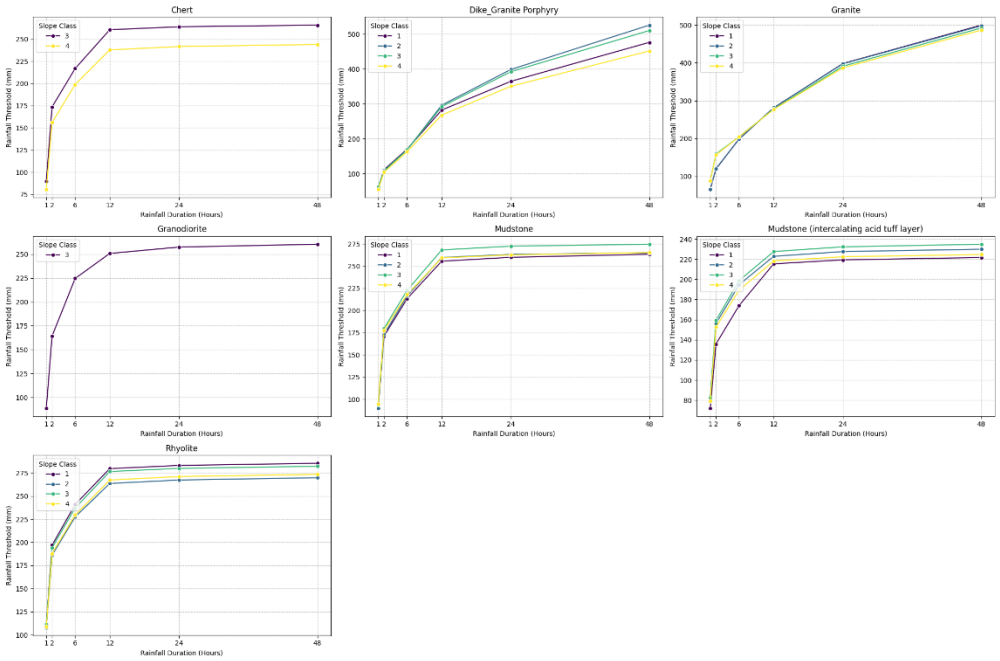

Figure 10. Rainfall intensity–duration threshold curves for different lithological units and slope classes. Each panel illustrates rainfall threshold variations across slope classes for specific rock types, including chert, dike granite porphyry, granite, granodiorite, mudstone, mudstone with intercalated acid tuff layers, and rhyolite.

5. Discussion

5.1. Rainfall Characteristics of the 2014 and 2018 Landslide Events

The rainfall analysis reveals two contrasting precipitation patterns associated with the 2014 Hiroshima and 2018 Western Japan landslide disasters. Although both events occurred within the same broader region of western Japan, the rainfall conditions and triggering mechanisms differed substantially.

The 2014 Hiroshima disaster was associated with a relatively short duration but extremely intense rainfall event. The most significant rainfall episode occurred between 19 and 20 August 2014, producing 376.05 mm of rainfall within approximately 40 hours. Such rainfall conditions are typical of localized convective storm systems capable of generating intense precipitation over short time periods. Similar rainfall characteristics were reported by previous studies investigating the Hiroshima disaster, which identified short-duration high-intensity rainfall as the primary trigger for numerous shallow landslides and debris flows [22,23]. These storms rapidly increase pore-water pressure in shallow soils, particularly in slopes composed of weathered granitic materials, which are highly susceptible to rainfall-induced failure [24,25].

Antecedent rainfall conditions may also have contributed to slope instability during the 2014 event. Several moderate rainfall episodes occurred in the days preceding the disaster, particularly between 8–10 August and 14–17 August. Antecedent rainfall is widely recognized as an important factor in landslide initiation because it increases soil moisture content and reduces the infiltration capacity of soils, thereby enhancing the susceptibility of slopes to subsequent intense rainfall [14,42].

In contrast, the 2018 Western Japan rainfall disaster was characterized by prolonged rainfall associated with a large-scale atmospheric circulation system. The rainfall event identified in this study lasted approximately 277.5 hours (about 11.5 days) between 26 June and 7 July 2018, producing more than 1000 mm of cumulative rainfall. Such long-duration rainfall events are typically linked to persistent atmospheric features such as stationary fronts and monsoonal moisture transport. Previous

 doi:10.20944/preprints202604.0975.v1

studies have shown that the 2018 disaster was caused by a stationary Baiu front interacting with continuous moisture supply from the Pacific Ocean, which resulted in widespread and persistent rainfall across western Japan [25,48].

Prolonged rainfall during this event led to progressive soil saturation and groundwater rise, ultimately reducing slope shear strength and triggering widespread landslides across the region. Similar mechanisms have been reported for other large-scale rainfall-induced landslide disasters associated with long-duration precipitation [16,47].

5.2. Intensity–Duration Rainfall Thresholds

The derived intensity–duration (I–D) rainfall thresholds further highlight the differences in rainfall triggering mechanisms between the two disasters. The threshold for the 2014 event indicates relatively high rainfall intensities for shorter durations, suggesting that landslide initiation was strongly controlled by rainfall intensity. This observation aligns with studies demonstrating that short-duration intense rainfall can rapidly generate pore-water pressure increases in shallow soil layers, leading to rapid slope failures [14,49].

In contrast, the 2018 rainfall threshold exhibits a flatter slope, indicating that rainfall duration played a more dominant role in triggering landslides during this event. Prolonged rainfall allows infiltration processes to progressively increase groundwater levels and soil moisture content, ultimately reducing slope stability over extended periods [42,47].

Comparison with previously proposed empirical rainfall thresholds also reveals that the derived relationships fall within the range of established landslide rainfall thresholds. For example, the global rainfall threshold proposed by Caine (1980) and the later refinement by Jibson (1989) represent widely recognized empirical relationships describing landslide-triggering rainfall conditions [45,49]. Similarly, satellite-based rainfall thresholds developed by Hong et al. (2005) and regional thresholds proposed for Japan by Saito et al. (2010) highlight the combined influence of rainfall intensity and duration in landslide initiation [46,47]. The thresholds derived in this study show similar trends but reflect the specific rainfall characteristics associated with the two disaster events.

5.3. Percentile-Based Rainfall Thresholds

The percentile-based rainfall threshold analysis provides further insights into rainfall conditions associated with landslide occurrence. The results indicate that rainfall thresholds generally increase with rainfall duration, particularly for higher percentile levels.

For the 2014 event, relatively high rainfall thresholds were observed for short-duration rainfall indices, indicating that intense rainfall bursts were required to trigger landslides. This pattern supports previous findings that the Hiroshima disaster was primarily driven by localized convective storms producing high rainfall intensities over short time periods [23].

In contrast, the 2018 disaster shows significantly higher rainfall thresholds for longer durations, particularly for 24-hour and 48-hour rainfall indices. These results highlight the dominant role of cumulative rainfall during prolonged precipitation events. Similar patterns have been reported in studies of typhoon and monsoonal rainfall events in Japan, where landslides are frequently associated with high cumulative rainfall over several days [25,47].

5.4. ROC-Based Evaluation of Rainfall Threshold Performance

The ROC-based threshold analysis provides an assessment of the predictive capability of rainfall thresholds for landslide occurrence. The results indicate moderate predictive performance for the 2014 event, with AUC values ranging from 0.52 to 0.61. This relatively lower performance may reflect the localized and highly variable nature of convective rainfall events, which often produce spatially heterogeneous rainfall patterns.

In contrast, the 2018 event shows higher AUC values ranging from 0.66 to 0.69, indicating better predictive capability of rainfall thresholds. The enhanced performance likely reflects the stronger relationship between cumulative rainfall and landslide occurrence during prolonged rainfall events.

 doi:10.20944/preprints202604.0975.v1

Previous studies have also reported that rainfall thresholds tend to perform better for long-duration rainfall events because these events produce more spatially uniform hydrological responses across large areas [14,42].

5.5. Influence of Slope Gradient and Lithology on Rainfall Thresholds for Landslide Initiation

The results indicate that landslide occurrence in the study area is governed by a complex interaction between topography, rainfall characteristics, and lithological conditions. Although slope gradient is traditionally considered one of the most important factors influencing landslide initiation, the present analysis shows that landslides can occur across a wide range of slope, with the largest landslide areas observed on moderately steep slopes. This pattern may reflect the influence of regolith thickness and weathering processes. Moderately steep slopes often accumulate thicker weathered material, which can become unstable during intense rainfall events. In contrast, very steep slopes may have thinner soil cover, limiting the size of potential landslides.

Rainfall threshold analysis further highlights the importance of rainfall duration and intensity. The relatively small variation in long-duration rainfall thresholds across slope classes suggests that prolonged rainfall plays a critical role in slope saturation and pore-water pressure buildup, which ultimately triggers landslides regardless of slope gradient. Lithological variations also exert strong control on rainfall thresholds. Rocks such as dike granite porphyry and granite, which commonly develop extensive joint networks and weathered zones, show relatively low rainfall thresholds, indicating higher susceptibility to rainfall-induced slope failure. In contrast, stronger lithologies such as rhyolite require higher rainfall intensities before slope failure occurs.

These findings support the concept that geological conditions influence landslide occurrence not only through direct mechanical properties but also by controlling on topographic evolution, weathering processes, and hydrological response of slopes.

5.6. Implications for Landslide Early Warning Systems

The results of this study highlight the importance of considering both rainfall intensity and duration when developing rainfall-based landslide early warning systems. Short-duration intense rainfall events can rapidly trigger shallow landslides, particularly in areas with highly weathered soils, whereas long-duration rainfall events can progressively destabilize slopes through cumulative infiltration and rising groundwater levels.

Therefore, landslide early warning systems should incorporate rainfall thresholds that account for both rainfall intensity and cumulative rainfall duration. Integrating multiple threshold approaches, including intensity–duration relationships, percentile-based thresholds, and ROC-based performance evaluation, may improve the reliability of landslide forecasting. Similar multi-threshold approaches have been recommended in previous landslide hazard studies [14,42].

Future research should also consider incorporating additional factors such as antecedent soil moisture, terrain characteristics, lithology, and land-use conditions, which can further improve the accuracy of landslide prediction models.

6. Conclusion

This study investigated rainfall conditions associated with two major landslide disasters in western Japan: the August 2014 and the July 2018 Hiroshima disaster events. These events were identified using an inter-event dry period approach applied to satellite-derived rainfall data. The results show clear differences in rainfall characteristics between the two disasters. The 2014 Hiroshima event was primarily triggered by short-duration, high-intensity rainfall, whereas the 2018 disaster resulted from prolonged rainfall accumulation over several days, producing more than 1000 mm of cumulative precipitation.

Rainfall threshold analysis using intensity–duration (I–D) relationships, percentile-based thresholds, and ROC-based evaluation demonstrated that both rainfall intensity and duration play critical roles in triggering landslides in western Japan. The derived thresholds are broadly consistent

 doi:10.20944/preprints202604.0975.v1

with previously reported rainfall thresholds but reflect the distinct meteorological characteristics of each event. ROC analysis indicates moderate to good predictive capability of the rainfall thresholds, particularly for the long-duration rainfall conditions associated with the 2018 disaster.

In addition to rainfall conditions, the analysis of terrain and geological factors revealed that landslide occurrence is governed by the interaction between slope gradient, lithology, and rainfall characteristics. Landslides were most frequently observed on moderate to steep slopes, while larger landslide areas tended to occur on moderately steep slopes, suggesting that slope gradient alone does not control landslide magnitude. Rainfall thresholds also varied slightly across slope classes, with short-duration rainfall thresholds generally increasing with slope gradient, whereas long-duration thresholds remained relatively consistent.

Lithological conditions aslo significantly influenced rainfall thresholds and landslide susceptibility. Granitic rocks and dike granite porphyry exhibited relatively low rainfall thresholds, reflecting their highly weathered nature and the presence of fracture networks that facilitate infiltration and slope failure. In contrast, stronger lithologies such as rhyolite required higher rainfall intensities to trigger landslides. These findings suggest that geological conditions influence landslide occurrence both directly through rock strength and indirectly by their control on slope morphology, weathering processes, and hydrological response.

Overall, this study demonstrates that rainfall-induced landslides in western Japan can be triggered by both intense short-duration rainfall and prolonged cumulative precipitation, even within the same geographic region. Integrating rainfall characteristics with topographic and lithological factors provides a more comprehensive framework for understanding landslide triggering mechanisms. Such an approach can improve rainfall-based landslide early warning systems and hazard assessment strategies in regions characterized by complex terrain, highly weathered slopes, and variable rainfall patterns.

Future research should focus on incorporating additional controlling factors, including antecedent soil moisture, detailed terrain parameters, and land-use conditions, to further enhance the accuracy and reliability of landslide prediction models.

Acknowledgments: This work was supported by JSPS KAKENHI Grant Numbers JP21K04605 and JP23K04337. The LiDAR data used in this study were obtained from a research project supported by JSPS KAKENHI Grant Number JP26900001.

Author Contributions: Kumari M. A. K: Writing-review and editing, Writing-original draft, Software, Methodology, Formal analysis, Data curation, Conceptualization. Tsuyoshi Wakatsuki: Writing-review and editing, Investigation, Supervision, Funding acquisition. Chiaki T. Oguchi: Writing-review and editing, Supervision. Osada Masahiko: Writing-review and editing, Supervision.

Conflicts of Interest: The authors declare that they have no known competing financial interest or personal relationships that could have appeared to influence the work reported in this paper.

 doi:10.20944/preprints202604.0975.v1

References

1. Huggins TJ, Chen K, Gong W and Yang L (2020) Infrastructural aspects of rain-related cascading disasters: A systematic literature review. International Journal of Environmental Research and Public Health 17:5175. https://doi.org/10.3390/ijerph17145175
2. Ebi KL, Vanos J, Baldwin JW, Bell JE, Hondula DM, Errett NA, Hayes K, Reid CE, Saha S, Spector J and Berry P (2021) Extreme weather and climate change: Population health and health system implications. Annual Review of Public Health 42:293–315. https://doi.org/10.1146/annurev-publhealth-012420-105026
3. Schuster RL and Fleming RW (1986) Economic losses and fatalities due to landslides. Environmental and Engineering Geoscience 23:11–28. https://doi.org/10.2113/gseegeosci.xxiii.1.11
4. Petley D (2012) Global patterns of loss of life from landslides. Geology 40:927–930. https://doi.org/10.1130/G33217.1
5. Sidle RC and Ochiai H (2006) Landslides: Processes, prediction and land use. John Wiley and Sons. https://doi.org/10.1002/9781118665954.fmatter
6. Kirschbaum DB, Adler RF, Hong Y, Huffman GJ and Lerner-Lam GJ (2010) A global landslide catalog for hazard applications: Method, results and limitations. Natural Hazards 52:561–575. https://doi.org/10.1007/s11069-009-9401-4
7. Guzzetti F, Mondini AC, Cardinali M, Fiorucci F, Santangelo M and Chang KT (2012) Landslide inventory maps: New tools for an old problem. Earth-Science Reviews 112:42–66. https://doi.org/10.1016/j.earscirev.2012.02.001
8. Hungr O, Leroueil S and Picarelli L (2014) The Varnes classification of landslide types, an update. Landslides 11:167–194. https://doi.org/10.1007/s10346-013-0436-y
9. Varnes DJ (1958) Landslide types and processes. In: Eckel EB (ed) Landslides and engineering practice. Highway Research Board, Special Report 29, pp 20–47.
10. Varnes DJ (1978) Slope movement types and processes. In: Schuster RL and Krizek RJ (eds) Landslides: Analysis and control. Transportation Research Board, Special Report 176, Washington DC, pp 11–33. ISSN: 0360-859X.
11. Iverson RM (2000) Landslide triggering by rain infiltration. Water Resources Research 36:1897–1910. https://doi.org/10.1029/2000WR900090
12. Highland LM and Bobrowsky P (2008) The landslide handbook: A guide to understanding landslides. United States Geological Survey. https://doi.org/10.3133/cir1325
13. Froude MJ and Petley DN (2018) Global fatal landslide occurrence from 2004 to 2016. Natural Hazards and Earth System Sciences 18:2161–2181. https://doi.org/10.5194/nhess-18-2161-2018
14. Guzzetti F, Peruccacci S, Rossi M and Stark CP (2007) Rainfall thresholds for the initiation of landslides in central and southern Europe. Meteorology and Atmospheric Physics 98:239–267. https://doi.org/10.1007/s00703-007-0262-7
15. Crosta GB and Frattini P (2008) Rainfall-induced landslides and debris flows. Hydrological Processes 22:473–477. https://doi.org/10.1002/hyp.6885
16. Guzzetti F, Peruccacci S, Rossi M and Stark CP (2008) The prediction of the onset of landslides: A review of rainfall thresholds and their use. Engineering Geology 99:31–59. https://doi.org/10.1016/j.enggeo.2008.02.002
17. Gariano SL and Guzzetti F (2016) Landslides in a changing climate. Earth-Science Reviews 162:227–252. https://doi.org/10.1016/j.earscirev.2016.08.011
18. Yasufuku N, Ochiai H and Matsushi Y (2021) Rainfall-induced landslides in Japan: Mechanisms and disaster mitigation approaches. Soils and Foundations 61:299–312.
19. White ID, Mottershead DN and Harrison SJ (1996) Environmental systems: An introductory text, 2nd edn. Chapman and Hall. ISBN: 0-7487-4081-3.
20. Segoni S, Piciullo L and Gariano SL (2018) A review of the recent literature on rainfall thresholds for landslide occurrence. Landslides 15:1483–1501. https://doi.org/10.1007/s10346-018-0966-4

 doi:10.20944/preprints202604.0975.v1

21. Osanai N, Shimizu T, Kuramoto K, Kojima S and Noro T (2010) Japanese early-warning system for debris flows and slope failures using rainfall indices with radial basis function network. Landslides 7:325–338. https://doi.org/10.1007/s10346-010-0229-5
22. Doshida S, Araiba K, Saito M and Kawabata D (2014) Slope collapses in Hiroshima City caused by heavy rain on August 20, 2014. Journal of the Japanese Society of Landslide Research 51:256–259. https://doi.org/10.3313/jls.51.256 (in Japanese).
23. Tsuchida T, Moriwaki T, Nakai S and Athapaththu AMRG (2019) Investigation and consideration on landslide zoning of multiple slope failures and debris flows of 2014 disaster in Hiroshima, Japan. Soils and Foundations 59:1085–1102. https://doi.org/10.1016/j.sandf.2018.12.012
24. Yoshihara N, Hattanji T, Doshida S, Tanaka Y and Furuichi T (2020) Geomorphological features of shallow landslides in hillslopes underlain by mixed rock of sandstone and mudstone: A case of heavy rainfall on August 20, 2014 in Hiroshima City, Japan. Tsukuba Geoenvironmental Sciences 16:15–25.
25. Wakatsuki T (2023) Recent sediment-related disasters triggered by extreme rainfall in western Japan and their geomorphological implications. Natural Hazards Review 24.
26. Ministry of Land Infrastructure Transport and Tourism (2014) Report of countermeasure of slope land disasters in Hiroshima triggered by heavy rainfall in August 2014. Accessed 4 Jun 2024. http://www.mlit.go.jp/river/sabo/H26_hiroshima/141031_hiroshimadosekiryu.pdf. (in Japanese).
27. Ministry of Land Infrastructure Transport and Tourism (n.d.) Official website. Accessed 6 Jul 2024. https://www.mlit.go.jp. (in Japanese).
28. Tsuji, H., Takayabu, Y. N., Shibuya, R., Kamahori, H., & Yokoyama, C. (2021). The role of free-tropospheric moisture convergence for summertime heavy rainfall in western Japan. Geophysical Research Letters, 48, e2021GL095030. https://doi.org/10.1029/2021GL095030
29. Ishizawa T and Danjo T (2019) Rainfall indices at estimated occurrence times of sediment disasters triggered by the July 2018 heavy rainfall. Journal of Disaster Research 14:1227–1235. https://doi.org/10.20965/jdr.2019.p1227
30. Uchida T, Shimizu T and Miyagi T (2011) Rainfall thresholds for shallow landslides in granitic mountain regions of Hiroshima, Japan. Engineering Geology 122:223–232.
31. Wang G, Sassa K and Fukuoka H (2015) Mechanisms of rainfall-induced shallow landslides in weathered granite slopes: Case study of the 2014 Hiroshima disaster, Japan. Engineering Geology 193:314–329.
32. Imam MH, Oguchi CT, Wakatsuki T and Ueda M (2019) Assessment of climate-induced degree of chemical weathering in some granite and granodiorite slopes of Japan. Modeling Earth Systems and Environment. https://doi.org/10.1007/s40808-019-00630-x.
33. Japan Meteorological Agency (2015) The query of past meteorological data. Accessed 19 Jan 2024. https://www.data.jma.go.jp. (in Japanese).
34. Yamamoto H (2016) Study of disaster prevention and characteristic elucidation of heavy rainfall and debris flow disaster in Hiroshima City, 20 August 2014. Grant-in-Aid for Scientific Research Report. https://kaken.nii.ac.jp/ja/grant/KAKENHI-PROJECT-26900001/
35. Guzzetti F, Reichenbach P, Cardinali M, Galli M and Ardizzone F (2005) Probabilistic landslide hazard assessment at the basin scale. Geomorphology 72:272–299. https://doi.org/10.1016/j.geomorph.2005.06.002
36. Van Westen CJ, Castellanos E and Kuriakose SL (2008) Spatial data for landslide susceptibility, hazard and vulnerability assessment: An overview. Engineering Geology 102:112–131. https://doi.org/10.1016/j.enggeo.2008.03.010
37. Fiorucci F, Ardizzone F, Cardinali M, Galli M, Guzzetti F and Reichenbach P (2011) Seasonal landslide mapping and estimation of landslide mobilization rates using aerial and satellite images. Geomorphology 129:59–70. https://doi.org/10.1016/j.geomorph.2011.01.013
38. Dunkerley D (2008) Identifying individual rain events from pluviograph records: A review with analysis of data from an Australian dryland site. Hydrological Processes 22:5024–5036. https://doi.org/10.1002/hyp.7122
39. Essien A, Dixon N and Ibsen M (2023) Rainfall thresholds for landslide initiation: A review of identification methods and uncertainty analysis. Landslides 20:245–264.

 doi:10.20944/preprints202604.0975.v1

40. He S, Wang J and Liu S (2020) Rainfall event–duration thresholds for landslide occurrences in China. Water 12:494. https://doi.org/10.3390/w12020494
41. Pradhan B and Lee S (2010) Delineation of landslide hazard areas using frequency ratio, logistic regression and artificial neural network model at the Pahang River Basin, Malaysia. Environmental Earth Sciences 59:227–238. https://doi.org/10.1007/s12665-009-0245-8
42. Brunetti MT, Peruccacci S, Rossi M, Luciani S, Valigi D and Guzzetti F (2010) Rainfall thresholds for the possible occurrence of landslides in Italy. Natural Hazards and Earth System Sciences 10:447–458. https://doi.org/10.5194/nhess-10-447-2010
43. Margottini C, Canuti P and Sassa K (eds) (2013) Landslide science and practice: Volume 2 – early warning, instrumentation and monitoring. Springer. ISBN: 978-3642314452
44. Pradhan B (2013) A comparative study on the predictive ability of decision tree, support vector machine and neuro-fuzzy models in landslide susceptibility mapping using GIS. Computers and Geosciences 51:350–365. https://doi.org/10.1016/j.cageo.2012.08.023
45. Jibson RW (1989) Debris flows in southern Puerto Rico. In: Schultz AP and Jibson RW (eds) Landslide processes of the eastern United States and Puerto Rico. Geological Society of America, pp 29–55. https://doi.org/10.1130/SPE236-p29
46. Hong Y, Adler RF and Huffman GJ (2007) Use of satellite remote sensing data in the mapping of global landslide susceptibility. Natural Hazards 43:245–256. https://doi.org/10.1007/s11069-006-9104-z
47. Saito H, Nakayama D and Matsuyama H (2010) Relationship between the initiation of a shallow landslide and rainfall intensity–duration thresholds in Japan. Geomorphology 118:167–175. https://doi.org/10.1016/j.geomorph.2009.12.016
48. Hashimoto R, Tsuchida T, Moriwaki T and Kano S (2020) Hiroshima Prefecture geo-disasters due to Western Japan torrential rainfall in July 2018. Soils and Foundations 60:283–299. https://doi.org/10.1016/j.sandf.2019.11.010
49. Caine N (1980) The rainfall intensity–duration control of shallow landslides and debris flows. Geografiska Annaler Series A Physical Geography 62:23–27. https://doi.org/10.1080/04353676.1980.11879996